NASA/TM–20250004056
NESC-RP-23-01949

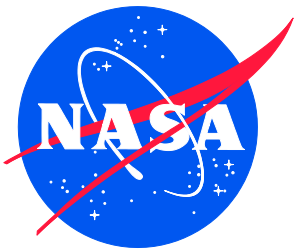

Docking Loads Due to Low-Gravity Propellant Motion

Tannen VanZwieten Cook (NESC) and John S. Bell
Langley Research Center, Hampton, Virginia

Justin McFatter
Johnson Space Center, Houston, Texas

Jing Pei, William J. Elke, and Brett R. Starr
Langley Research Center, Hampton, Virginia

April 2025

NASA STI Program Report Series

Since its founding, NASA has been dedicated to the advancement of aeronautics and space science. The NASA scientific and technical information (STI) program plays a key part in helping NASA maintain this important role.

The NASA STI program operates under the auspices of the Agency Chief Information Officer. It collects, organizes, provides for archiving, and disseminates NASA's STI. The NASA STI program provides access to the NTRS Registered and its public interface, the NASA Technical Reports Server, thus providing one of the largest collections of aeronautical and space science STI in the world. Results are published in both non-NASA channels and by NASA in the NASA STI Report Series, which includes the following report types:

- TECHNICAL PUBLICATION. Reports of completed research or a major significant phase of research that present the results of NASA Programs and include extensive data or theoretical analysis. Includes compilations of significant scientific and technical data and information deemed to be of continuing reference value. NASA counterpart of peer-reviewed formal professional papers but has less stringent limitations on manuscript length and extent of graphic presentations.

- TECHNICAL MEMORANDUM. Scientific and technical findings that are preliminary or of specialized interest, e.g., quick release reports, working papers, and bibliographies that contain minimal annotation. Does not contain extensive analysis.

- CONTRACTOR REPORT. Scientific and technical findings by NASA-sponsored contractors and grantees.

- CONFERENCE PUBLICATION. Collected papers from scientific and technical conferences, symposia, seminars, or other meetings sponsored or co-sponsored by NASA.

- SPECIAL PUBLICATION. Scientific, technical, or historical information from NASA programs, projects, and missions, often concerned with subjects having substantial public interest.

- TECHNICAL TRANSLATION. English-language translations of foreign scientific and technical material pertinent to NASA's mission.

Specialized services also include organizing and publishing research results, distributing specialized research announcements and feeds, providing information desk and personal search support, and enabling data exchange services.

For more information about the NASA STI program, see the following:

- Access the NASA STI program home page at http://www.sti.nasa.gov

- Help desk contact information:

https://www.sti.nasa.gov/sti-contact-form/
and select the "General" help request type.

NASA/TM–20250004056
NESC-RP-23-01949

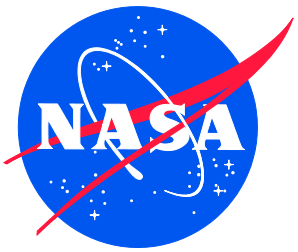

Docking Loads Due to Low-Gravity Propellant Motion

Tannen VanZwieten Cook (NESC) and John S. Bell
Langley Research Center, Hampton, Virginia

Justin McFatter
Johnson Space Center, Houston, Texas

Jing Pei, William J. Elke, and Brett R. Starr
Langley Research Center, Hampton, Virginia

National Aeronautics and
Space Administration

Langley Research Center
Hampton, Virginia 23681-2199

April 2025

Acknowledgments

The authors would like to acknowledge the contributions from technical consultants Sasan Armand, Carlos Roithmayr, Joel Sills, and John Wall. In addition, the support from program analyst Linda Moore, project coordinator Lynne Hartman, planning and control analyst Linda Burgess, and technical editors Christa Hahn and Dee Bullock.

The NESC assessment team would also like to thank Timothy Barth, NESC Integration Office (KSC); Robert Beil, NESC Integration Office (KSC); Elliott Cramer, NESC Chief Engineer (LaRC); Chris D'Souza, NASA Technical Fellow, GNC (JSC); Steve Gentz, NESC Chief Engineer (MSFC); Heather Koehler, NASA Technical Fellow, Flight Mechanics (MSFC); Joel Sills, NESC Chief Engineer (JSC); and Eric Stewart, SLS Sub-Discipline Lead Engineer for Loads and Dynamics (MSFC), for their valuable contributions as peer reviewers.

Available from:

NASA STI Program / Mail Stop 050
NASA Langley Research Center
Hampton, VA 23681-2199

Table of Contents

1.0 Problem Description and Assumptions 1
2.0 Analysis 2
2.1 Fluid Mechanics Analysis 4
2.2 Impulse/Momentum Analysis 6
2.3 Dynamic Simulation with Slosh Particle Model in Simulink 8
2.4 Chaser/Target Vehicle Docking in Adams with the NDSB2 14
2.4.1 Docking Simulation Setup 14
2.4.2 Docking Simulation Results 15
2.5 Summary of Results 19
3.0 Findings, Observations, and NESC Recommendations 20
3.1 Findings 20
3.2 Observations 21
3.3 NESC Recommendations 22
4.0 Alternate Technical Opinion(s) 22
5.0 Other Deliverables 22
6.0 Recommendations for the NASA Lessons Learned Database 22
7.0 Recommendations for NASA Standards, Specifications, Handbooks, and Procedures 22
8.0 Definition of Terms 23
9.0 References 23

List of Figures

Figure 2.0-1. NDSB2 Active 3
Figure 2.0-2. NDSB2 Passive 3
Figure 2.0-3. NDSB2 Docking Timeline 4
Figure 2.1-1. Absolute Velocities of the Chaser and Target Vehicles in the Fluid Mechanics Analysis 5
Figure 2.1-2. Propellant Flow Pattern 5
Figure 2.1-3. Docking (SCS) Force (left) and Slosh Forces (right) 6
Figure 2.2-1. Slosh Particle Impacts LOX Tank Forward End During Docking 7
Figure 2.2-2. Total shear (top) and axial (bottom) impulses for the second collision 8
Figure 2.3-1. Particle Positions in the chaser vehicle Tanks Through the Simulation Duration 10
Figure 2.3-2. Sample Chaser/Target Vehicle Relative Position (Left) and Velocity (Right) (Desired and Actual) 10
Figure 2.3-3. Initial Particle Positions with Highlighted Lateral RSS Docking Misalignment Requirement Success (Blue) and Failure (Red) 11
Figure 2.3-4. Relative Lateral RSS Misalignments of the Docking Interface with RCS Thruster Minimum On-Times of 50 ms 12
Figure 2.3-5. Distribution of the Combined Particle Slosh Force where the Force was Sustained During the Beginning of the Capture Sequence 12
Figure 2.3-6. Relative Lateral RSS Misalignments of the Docking Interface Considering all Thruster Minimum On-times 13
Figure 2.4-1. NDSB2 Dynamics Model 14
Figure 2.4.2-1. Lateral and Wobble Misalignment ICCs with Slosh Enabled 15

Figure 2.4.2-2. Linear Actuator Lower Joint Motion with Slosh Enabled 16
Figure 2.4.2-3. Soft Capture Loads as a Percentage of Limit Load 17
Figure 2.4.2-4. HCS Engagement Loads as a Percentage of Limit Load 17
Figure 2.4.2-5. Predicted Soft Capture Loads 18
Figure 2.4.2-6. Severe Misalignment Case with Improper Guide Meshing 19
Figure 2.5-1. Propellant Slosh Load Predictions from Multiple Methods 20

List of Tables

Table 2.3-1. Maximum Relative Changes of Docking Interface Lateral Offsets across all Scenarios and Monte Carlo Results 13
Table 2.4.2-1. Docking Success Summary 18

Nomenclature

ρ	Fluid density
3D	Three Dimensional
Adams	Automatic Dynamic Analysis of Mechanical Systems
B2	Block 2
CFD	Computational Fluid Dynamics
CM	Center of Mass
DoF	Degree of Freedom
FEM	Finite Element Model
F_x	Axial slosh force
g	Gravity
GNC	Guidance, Navigation, and Control
HCS	Hard Capture System
ICPS	Interim Cryogenic Propulsion Stage
IDD	Interface Definition Document
IDSS	International Docking System Standard
ISS	International Space Station
LCH_4	Liquid Methane
LOX	Liquid Oxygen
M2M	Moon to Mars
MPCV	Multi-Purpose Crew Vehicle
m/s	meters/second
ms	milliseconds
N	Newton
NDS	NASA Docking System
NDSB2	NASA Docking System Block 2
NESC	NASA Engineering and Safety Center
NRHO	Near-Rectilinear Halo Orbit
RCS	Reaction Control System
ROM	Rough order of magnitude
RSS	Root-Sum-Square
s	second
SCS	Soft Capture System
SE&I	Systems Engineering and Integration
STARS	Space Transportation Analysis and Research Simulation
v	velocity
VRDM	Vehicle Relative Dynamic Motion

Abstract

Slosh dynamics can have a detrimental effect on spacecraft approach, pointing, and docking in a low-gravity (low-g) environment when there are significant amounts of both propellant mass and open tank volume. This report uses four methods to estimate chaser/target vehicle docking loads that consider the effect of the chaser vehicle propellant movement and assumes a 50% full liquid oxygen (LOX)-Methane (LCH_4) dual tank configuration. All the models leveraged assumptions on the propellant slosh behavior that have not been validated since the dynamic behavior of fluid in a low-g environment is an area of active research with limited data for model validation.

The first two analysis methods were intended to provide rough order of magnitude (ROM) loads estimates — one based on fluid mechanics and one on impulse momentum. The third method, a multi-body dynamic simulation, was developed which incorporated single particle mechanical slosh models for LOX and LCH_4. The slosh model consists of a free-moving particle within a constraint surface with penalty method-based contact dynamics and an inert particle that augments the mass properties of the spacecraft. The parameters of the slosh model are tuned with computational fluid dynamics (CFD) simulations of a representative scenario. The simulation framework allowed for the Monte Carlo analysis of the chaser vehicle approach in order to evaluate the associated slosh loading before, during, and after docking. The fourth method used the dynamic simulation states at first contact with the target vehicle as initial conditions for a high-fidelity Adams[1] model that included the NASA Docking System Block 2 (NDSB2) mechanism. The inclusion of this fourth analytical method permits a more detailed evaluation of potential challenges with docking beyond basic loads calculations, including the impact of misalignments on docking, linear actuator stroke length limitations, and the potential for damaging contact during docking.

The impact of post-contact propellant motion on loads for the docking profile evaluated appeared to be minor compared to the impact of misalignments due to the assumed controller and actuator design. Only the high-fidelity Adams model that included the NDSB2 docking mechanism was able to identify missed capture cases, with and without propellant motion, and scenarios that would be potentially damaging to the NDSB2 docking mechanism.

1.0 Problem Description and Assumptions

There is concern regarding the potential of having excessive loads when chaser/target vehicles dock due to propellant motion in a low-g environment. The analysis described herein presents the

[1] Adams is a multibody dynamics simulation provided by Hexagon, formerly MacNeal-Schwendler Corporation (MSC) Software.

expected loading impacts due to the motion of a large chaser vehicle propellant mass during and just after docking. The chaser vehicle tanks were assumed to be a 50% full LOX-LCH_4 configuration and the target vehicle is assumed to be rigid (no propellant slosh). In addition, the corresponding chaser vehicle propellant mass was assumed to be significantly greater than the mass of the target vehicle.

The scope of work conducted was to provide a loads estimate by completing the following analyses:

1. Hand calculations with basic assumptions on fluid location before and after docking (a similar analysis is documented in ref. 4). This method evaluates forces based on assumed flow rates when the propellant is redirected by the forward end of the tank.
2. Generalized impulse-momentum analysis with assumptions:
    - Planar motion: out-of-plane motion of the slosh particles or the chaser/target vehicle rigid bodies is not considered
    - The chaser vehicle approaches a stationary target vehicle
    - Inelastic collision with no subsequent slipping between vehicles (vehicles move as a single body after the collision)
3. Simulation of the chaser vehicle final maneuver and docking to the target vehicle with inclusion of low-g slosh particle model to evaluate loads:
    - Calibrate and integrate particle models into existing chaser vehicle 6 degree-of-freedom (6-DoF) model
    - Dynamically model the chaser vehicle final maneuver and docking with the target vehicle in Simulink with the inclusion of thrusters/GNC models
4. Simulation of the docking mechanism due to its potential for dynamic coupling and the complex nature of its constraints. Slosh loads can be within docking mechanism load limits but can cause misalignments or problematic coupled system dynamics that can result in failure to dock.

2.0 Analysis

This section summarizes the analysis performed and results from the chaser vehicle approach maneuver and docking with the target vehicle. All analyses reference the same approach trajectory.

The NDSB2 is an International Docking System Standard (IDSS)-compatible docking system, with the active component shown in Figure 2.0-1 and the passive component (which will be assumed to be used by the target vehicle) shown in Figure 2.0-2. Figure 2.0-3 shows the timeline of NDSB2 soft capture operations through hook closure using this parameter set established for Artemis III (HLS-MPCV). Aside from the interface load limits, which apply to all docking scenarios and are defined in the IDSS [ref. 2], the docking mechanism performance and limitations discussed in this report are specific to NDSB2.

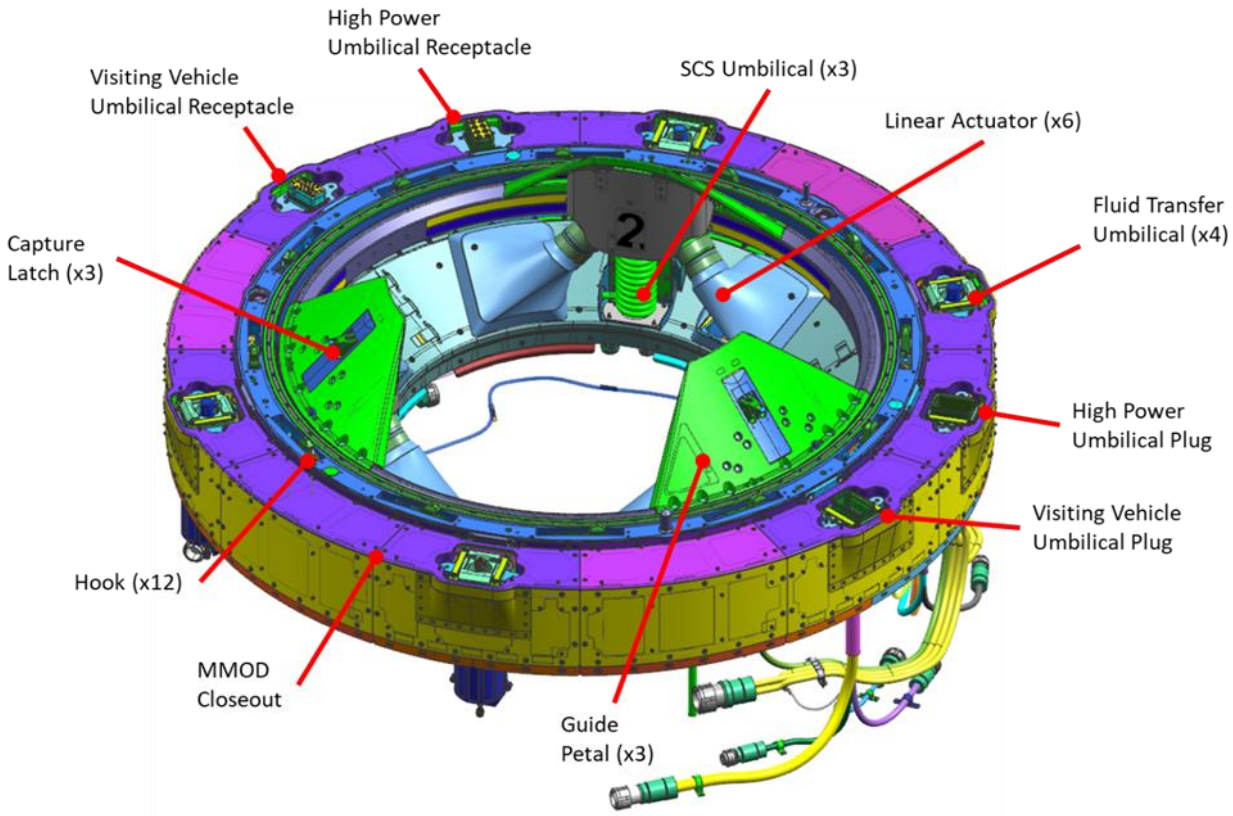

Figure 2.0-1. NDSB2 Active

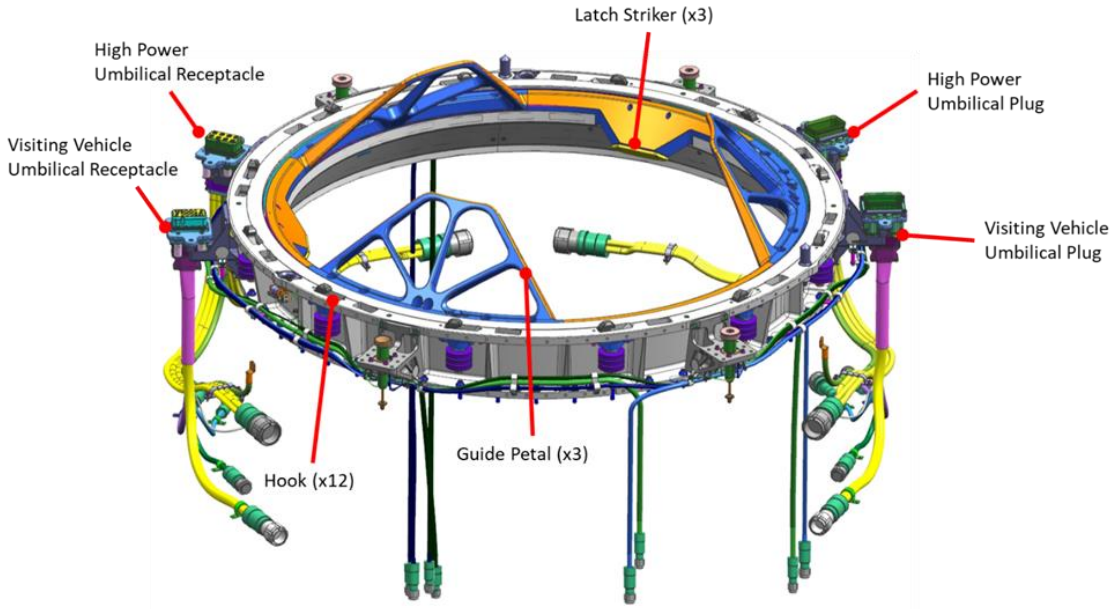

Figure 2.0-2. NDSB2 Passive

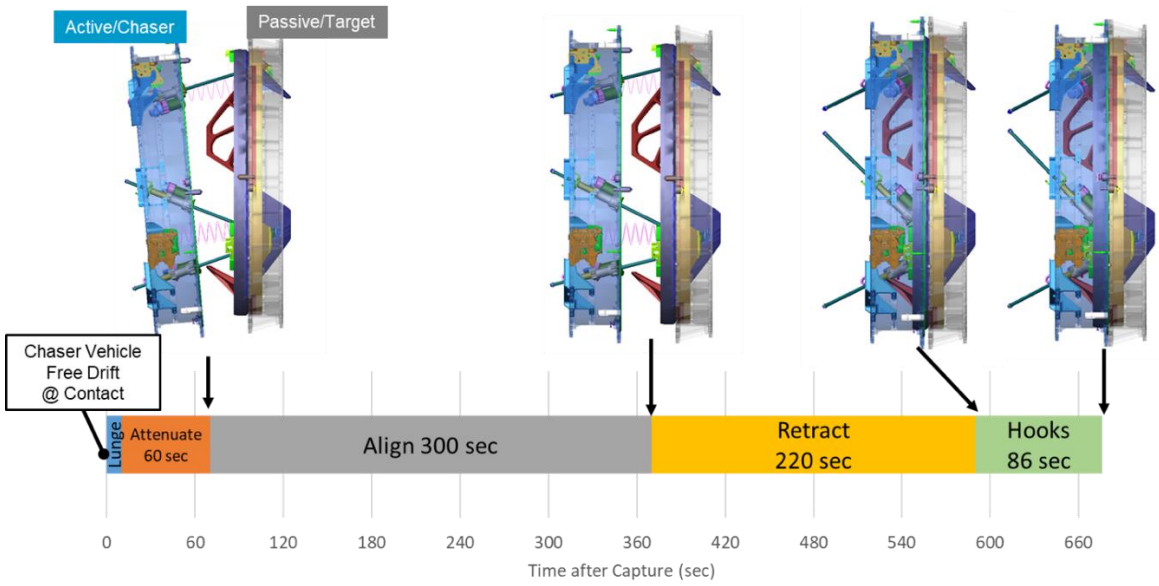

Figure 2.0-3. NDSB2 Docking Timeline [ref. 5]

2.1 Fluid Mechanics Analysis

The fluid mechanics approach estimates the forces imparted from the chaser vehicle propellant on the LOX and LCH_4 tank walls by making assumptions on the fluid behavior. This approach followed the method used for Artemis II Multi-Purpose Crew Vehicle (MPCV)/Interim Cryogenic Propulsion Stage (ICPS) separation analysis under NESC-TI-12-00766, "Exploration Systems Independent Modeling and Simulation" [ref. 4]. Two tanks are onboard the chaser vehicle: one with LOX; and the other with LCH_4. It is assumed that at the time of docking with the target vehicle, approximately 50% of each of these propellants are expected to be depleted, leaving the other 50% of the tanks as unfilled space permitting propellant movement. As the chaser vehicle approaches the target vehicle, the spacecraft slows and docks, causing the propellants to move towards the tank forward bulkheads. The fluid mechanics approach leverages conservation of momentum to calculate the resulting velocity of the docked pair. Using the spacecraft pre- and post-docking velocities, the relative velocity between the propellant in the tanks and the spacecraft is obtained. It was assumed that the SCS imparts a maximum force on the chaser vehicle of 2150 Newtons (N) during capture which results in the chaser vehicle and the target vehicle equalizing to the post-capture velocity (see Figure 2.1-1).

The left plot in Figure 2.1-1 provides the absolute velocities of the chaser and target vehicles. At time (t) = 0, the target vehicle has zero velocity until contact is made. During the soft docking phase, their relative motion is arrested, and after this point the combined chaser/target system moves with a velocity as indicated by the "captured" line in Figure 2.1-1. The captured velocity is increased by the propellant slosh effects (shown in the right plot of Figure 2.1-1). Note the that the time scale on the right subfigure is orders of magnitude larger than the left subfigure.

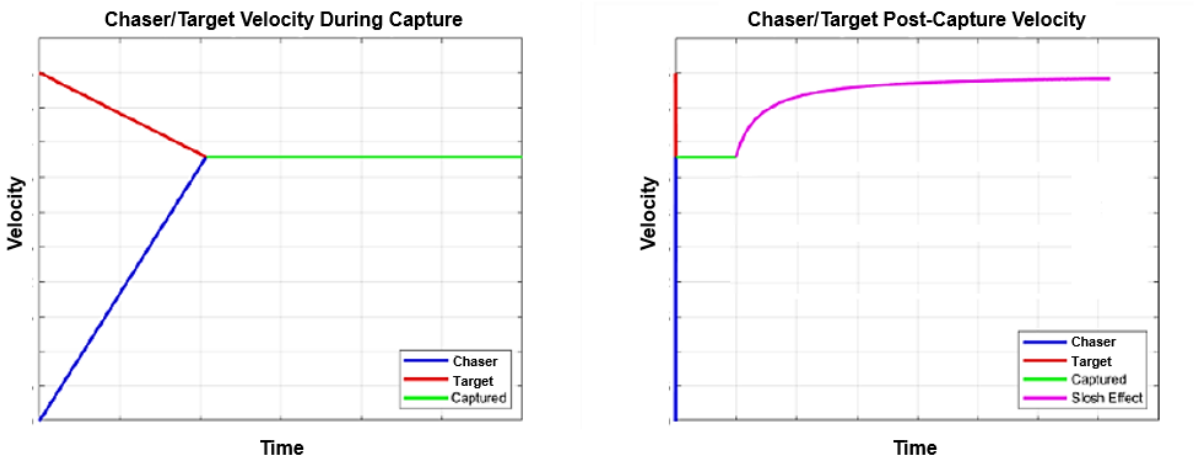

Figure 2.1-1. Absolute Velocities of the Chaser and Target Vehicles in the Fluid Mechanics Analysis

The initial position of the propellants inside their tanks is assumed to be in equilibrium where the propellants are in a crescent-like shape at the ends of the tanks. The equilibrium shape is a function of the liquid density, surface tension, and Bond number. This fluid equilibrium distribution is based on existing data from 0-g slosh tests [ref. 6] performed on the International Space Station (ISS). During capture, the chaser vehicle slows, but its propellant continues to move at the chaser vehicle pre-approach velocity. This results in the propellants in the aft end of the tanks flowing forward into the tank forward ends. The flow patterns assumed for the fluid mechanics analysis are also based on flow patterns observed in the ISS 0-g slosh tests. Figure 2.1-2 shows the assumed post capture propellant flow pattern.

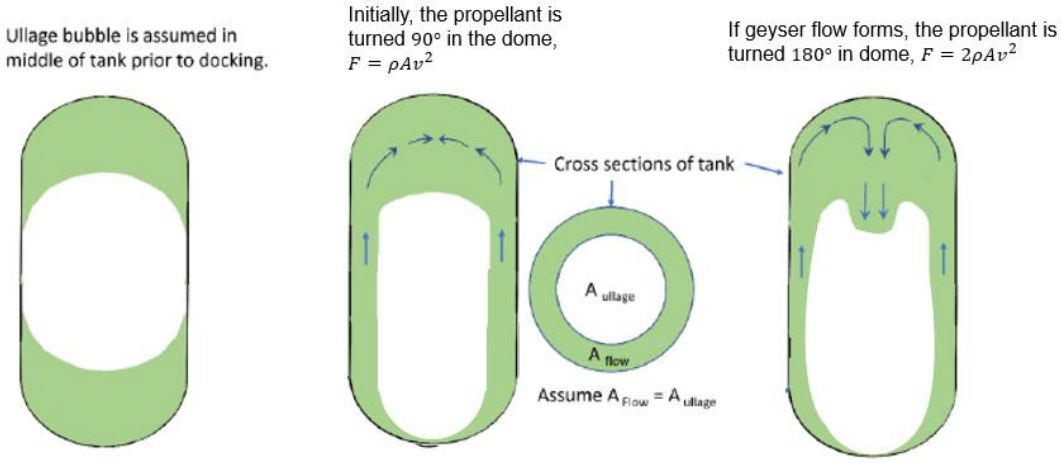

Figure 2.1-2. Propellant Flow Pattern

The estimates of the chaser vehicle propellant forces on the tanks were calculated using equations for fluid flow onto a curved plate. These equations utilize the fluid density, ρ; the cross-sectional area of the flow, A; and the fluid flow velocity, v. The axial slosh force, F_x, is a function of the mass flow rate and change in flow velocity or direction.

- For flow that comes to a stop in the tank forward end, $F_x = \rho A v^2$.
- For flow that reverses direction in the tank forward end (i.e., geyser-type flow), $F_x = 2\rho A v^2$.

Flow reversal in a purely axial direction maximizes the force imparted from the propellant on the tank walls. A slight misalignment may cause lateral loads that are not accounted for in this analysis. During soft capture, the SCS applies its maximum axial force. This is shown on the left side of Figure 2.1-3. Due to the distance the propellant in the tank aft end must travel to reach the tank forward end and have its flow velocity and direction reversed, the slosh force occurs well after capture, as shown on the right side of Figure 2.1-3. The slosh force peaks and then rapidly decreases as the combined chaser/target vehicle system accelerates and the tank relative flow velocity decreases.

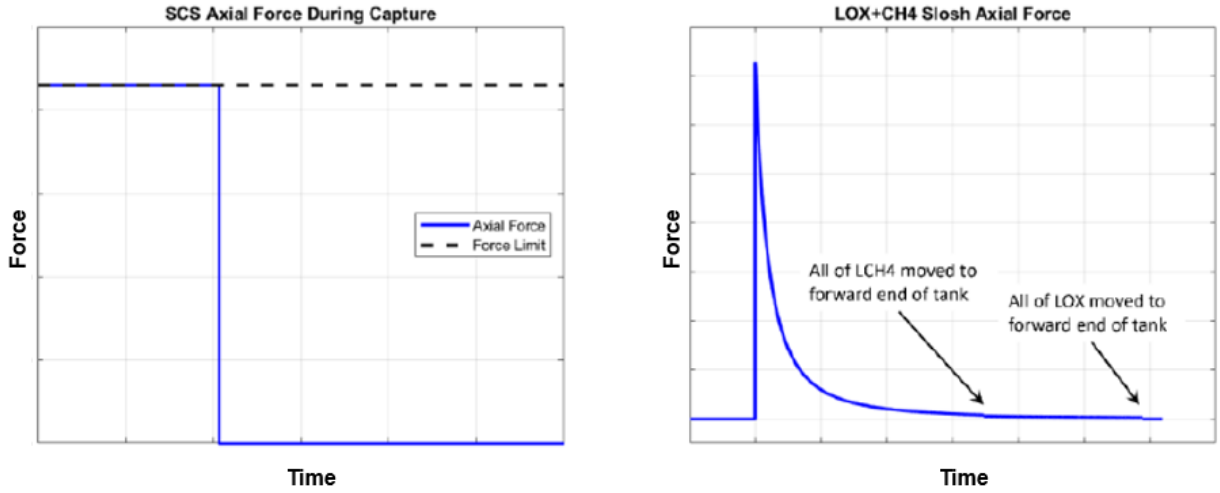

Figure 2.1-3. Docking (SCS) Force (left) and Slosh Forces (right)

2.2 Impulse/Momentum Analysis

The impulse/momentum analysis relies on Kane's theory of generalized impulse and momentum in the treatment of collision dynamics [ref. 3]. This method assumes that the dry chaser and target vehicles can be analytically represented as rigid bodies with distributed mass, and the propellants can be represented as single particles. In this analysis, only the furthest-aft tank is modeled. This one-tank approximation maximizes the moment arm about the docking interface, thus being a conservative assumption. Furthermore, both propellant masses are conservatively assumed to be combined into a single particle in which the entire propellant mass contributes to the slosh force. Two separate collisions are modeled corresponding to the accelerations imparted by the chaser vehicle approach trajectory and impact with the target vehicle: first, the braking gate results in an inelastic collision between the particle and the tank forward end; and second, a collision between the combined chaser vehicle/particle system and the target vehicle. Both collisions assume planar motion, and slosh and docking loads are estimated from the impulse exchanged between the colliding bodies.

Kane's method of using generalized impulse and momentum to treat collision dynamics assumes that the collisions take place across a short duration of time, which is an assumption inherently not carried by the fluid mechanics approach. This also means that Kane's method should serve as an assumed 'upper bound' on the slosh force estimation as fluid exhibits significantly more damping during a collision than a rigid body and the collision occurs more gradually. The force imparted from the propellant particles on the chaser vehicle rigid body in this first collision under nominal conditions was obtained. The collision duration was assumed to be relatively short and resulted in a force magnitude much larger than the estimate provided by the Fluid Mechanics approach.

The second collision is between the combined chaser vehicle/particle system and the target vehicle. Like the fluid mechanics approach, the NDSB2 actuator system was assumed to impart a constant force on the chaser vehicle during soft docking. In Figure 2.2-1, the reaction forces R1, R2, and R4 are found to be of low, medium, and high magnitude, respectively. R4 is greater than R2 because of the propellant offset and because the center of gravity (CG) of target vehicle was biased in the n_1 direction.

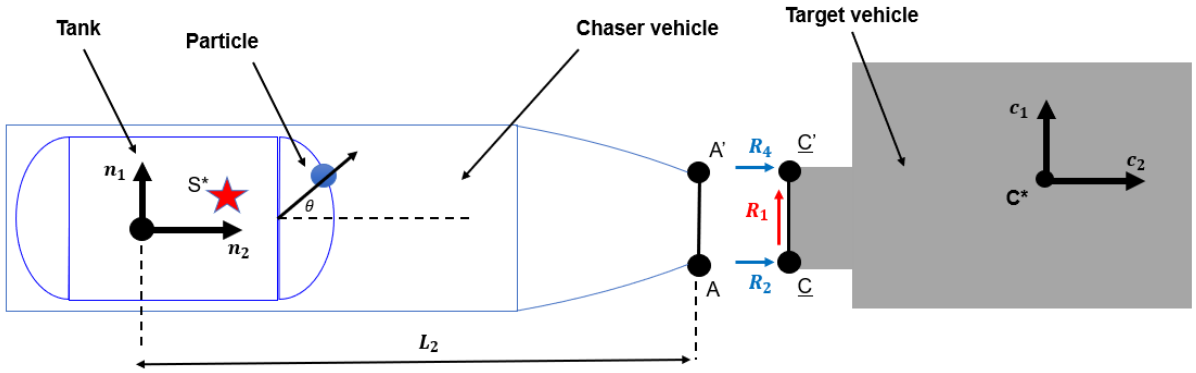

Figure 2.2-1. Slosh Particle Impacts LOX Tank Forward End During Docking

A Monte Carlo analysis was performed to determine the bounds of the shear impulses (R_1 in Figure 7.2-1) and the total axial impulses ($R_4 + R_2$ in Figure 2.2-1) for the second collision. The parameter dispersions are applied to: the particle axial velocity (u_2), the particle lateral velocity (u_1), the chaser vehicle angular rate (u_5), and the particle impact angle relative to the tank centerline (θ).

The particle axial velocity, u_2, is the absolute velocity of the particle prior to the first collision. The bounds on u_2 are selected based on the approach profile. The lateral velocity (u_1) bounds were selected based on engineering judgement.

The chaser vehicle angular rate, u_5, was based on the observed maximum spacecraft rotation at the time of docking from the dynamic simulation with the slosh particle model. The particle impact angle relative to the tank centerline, θ, is the angle at which the particle contacts the curved tank surface, as shown in Figure 2.2-1. It is assumed that the particle can come in contact with the entirety of the forward dome, resulting in bounds of $\pm\pi/2$ radians.

The NDSB2 has range of motion limits that used the force-time profile to calculate impulse limits. The docking system has both shear and axial impulse limits. Monte Carlo analysis results are provided in Figure 2.2-2 with the limits represented by the red lines.

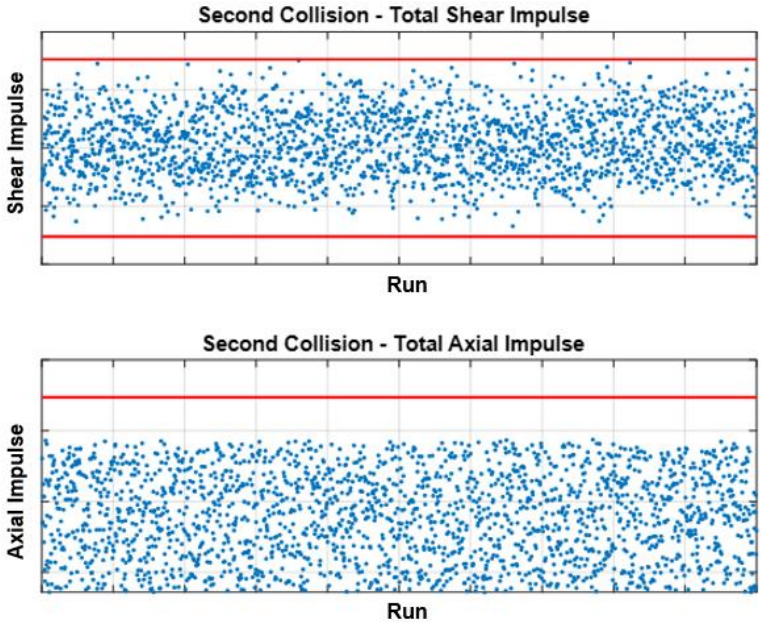

Figure 2.2-2. Total shear (top) and axial (bottom) impulses for the second collision

No exceedances of the shear or axial impulse limits were observed. However, when increasing the chaser vehicle angular rate to the International Docking System Standard (IDSS) Interface Definitions Document (IDD) limit, exceedances were observed in the shear channel.

2.3 Dynamic Simulation with Slosh Particle Model in Simulink

The chaser vehicle dynamics simulation included the spacecraft rigid body dynamics, mechanical slosh particle models for LOX and LCH_4, representative models for the thrusters, and flight control system. During approach, perfect navigation was assumed (i.e., no sensor models). Both the chaser and target vehicles were assumed to reside on a 9:2 Near Rectilinear Halo Orbit (NRHO)[2], whereby only relative motions are relevant to the analysis herein. To maximize unstable relative dynamics and gravity gradient torque, the Proximity Operation and Docking sequence was assumed to occur near the point in NRHO that is furthest from the Moon (i.e., apolune). The simulation was developed in Space Transportation Analysis and Research Simulation (STARS), a Simulink-based tool which can support Monte Carlo analysis. This tool was developed at NASA LaRC in 2007, primarily in support of the Ares-IX flight program and continues to be used for the Artemis Program verification and validation.

The controller was designed to compute the desired torque and force based on the errors between the true and desired vehicle 6-DoF states, and the controller bandwidth was set to avoid potential excitation of the chaser vehicle propellant slosh or solar array modes. To estimate the effects of docking on the chaser vehicle, the force from the docking system on the chaser vehicle was consistent with the constant force assumed in the previous two analyses. The force was applied to the chaser vehicle after initial contact when the relative axial distance between the docking interfaces between the chaser and the target equals 0.

[2] https://ntrs.nasa.gov/api/citations/20200002920/downloads/20200002920.pdf

The slosh particle model is discussed in ref. 9. A particle model was chosen over CFD simulations because of computational efficiency, which allowed for several thousand simulation runs to be executed. The slosh particle model formulation is a low-order mechanical model for each tank that attempts to characterize the propellant forces and motions while neglecting higher-order slosh modes and droplet formations. The moving propellant is assumed to be a lumped mass (i.e., particle, or a cohesive slug of propellant) and the contact model is assumed to be critically damped. These assumptions break down when there are different fluid initial conditions, increased time horizons, and dynamic tank motions. The slosh particle model fixes a portion of the propellant to the center of the constraint surface (inert) and permits a particle representing the remaining propellant mass to translate freely within a constraint surface boundary. When the moving particle contacts or exits the constraint surface, a restoring force is computed via penalty method-based contact dynamics. The particle moment to calculate the docking loads is the torque about the docking interface caused by the combined net force from both the LOX and LCH_4 particles. In other words, torque is calculated by the cross product of (1) the position vector beginning at the docking interface and terminating at the point of contact, and (2) the force vector due to contact between the particle and the constraint surface.

Three sets of Monte Carlo analyses were performed. Initially, $2^{13} = 8192$ cases were generated which included starting positions for each of the particles within a bounding cube with dimensions equal to the constraint surface ellipsoid diameters. Cases in which one of the two particles fell outside the constraint surfaces were removed. After this down-select, each analysis set consisted of 2228 individual runs. The first was a simulation using the dry mass of the chaser vehicle with centered inert propellant masses. This Monte Carlo analysis set assessed the variability of results with varying minimum thruster on-times (50, 100, 150 ms). These results served as the baseline. The second Monte Carlo analysis randomly distributed the inert propellant positions within the tanks. The purpose of this simulation was to examine the effects of a significant center of mass (CM) misalignment. The third Monte Carlo analysis included the propellant slosh particle model, where a portion of the propellant was given a random initial position and was subsequently free to translate and interact with the tank walls. Figure 2.3-1 shows an example of the particle behavior during a simulation. The chaser vehicle tanks are shown and the ellipsoidal volumes within them represent the model constraint surfaces, the size of which varies based on the tank fill level. When the particle exits the constraint surface, it will be pulled back by a contact model with CFD-tuned parameters. This interaction was intended to model the fluid's interaction with the tank wall, which will increase as a larger quantity of fluid pushes towards the wall. Figure 2.3-2 provides an example of the spacecraft's relative position (left) and velocity (right) compared to that of the desired approach profile. Deviations from the desired approach velocity can be observed as the propellant slosh particles interact with the constraint surface boundary. The controller corrects the spacecraft relative velocity with the desired approach velocity well in advance of the simulated docking.

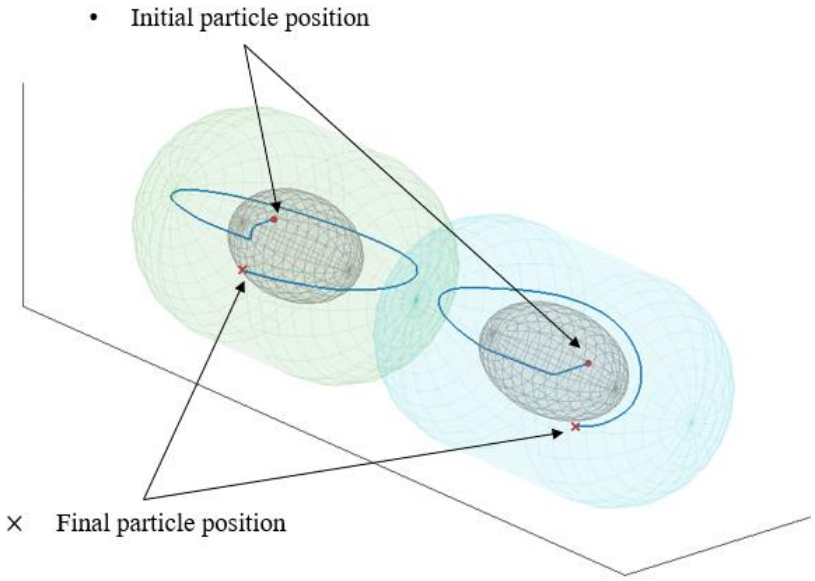

Figure 2.3-1. Particle Positions in the chaser vehicle Tanks Through the Simulation Duration

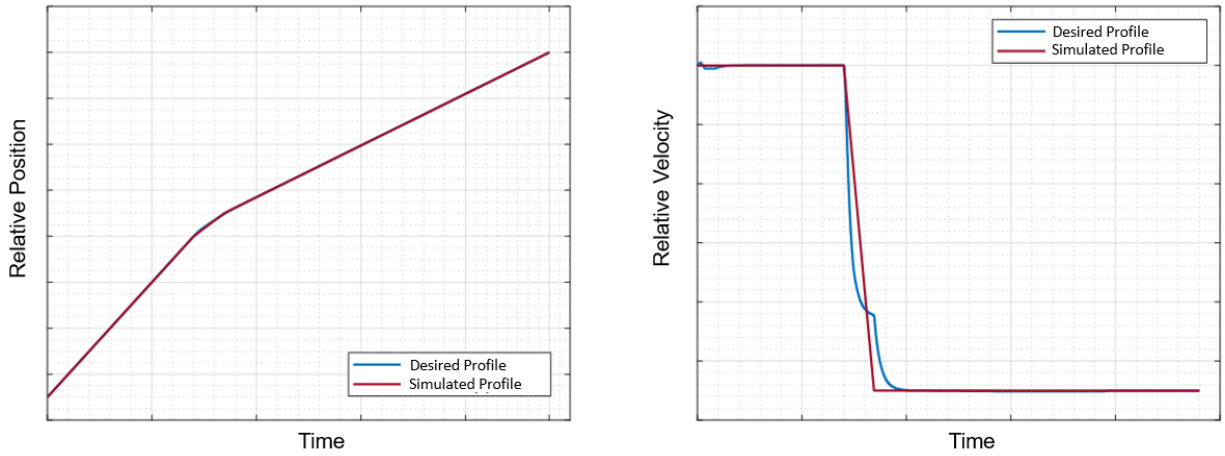

Figure 2.3-2. Sample Chaser/Target Vehicle Relative Position (Left) and Velocity (Right) (Desired and Actual)

During the chaser vehicle approach maneuver, results were obtained for the Monte Carlo analysis with slosh enabled:

- The maximum combined particle force magnitude on the spacecraft (both LOX and LCH_4 propellant acting at a specific point in time).
- The maximum torque on the spacecraft about the docking interface from both particles (i.e., LOX and LCH_4 propellant acting at a specific point in time).
- Cases were observed where the propellant relative velocity due to the braking maneuver was sustained until docking.

At the point of docking, it was found that there was low correlation between initial particle position and the chaser vehicle's misalignment at the docking interface. Figure 2.3-3 provides the initial particle positions in the slosh enabled Monte Carlo analysis runs highlighted according to the success (blue) or failure (red) of the lateral root-sum-square (RSS) docking interface misalignment meeting IDSS requirements. The lateral RSS docking misalignment is the driver for overall

docking success. The figure has the constraint surfaces artificially moved closer together for figure clarity.

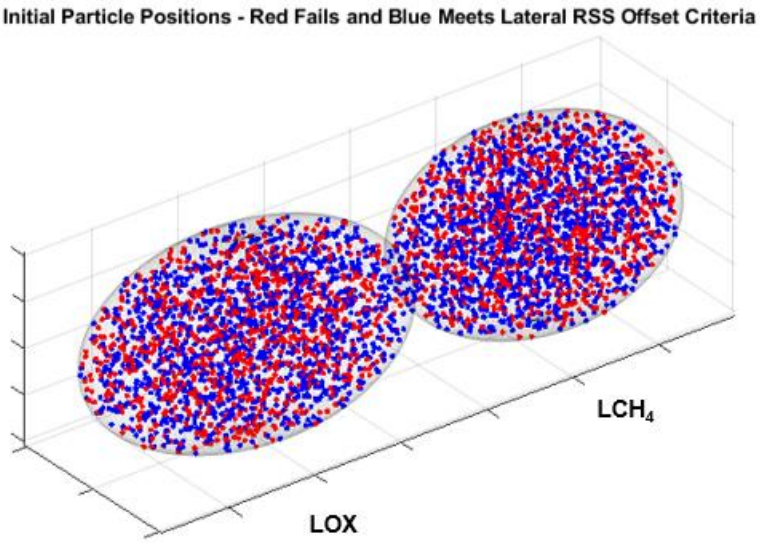

Figure 2.3-3. Initial Particle Positions with Highlighted Lateral RSS Docking Misalignment Requirement Success (Blue) and Failure (Red)

Figure 2.3-4 provides the Monte Carlo results for relative lateral displacements with minimum RCS thruster on-time of 50 milliseconds (ms). The maximum offset with slosh enabled was 48% greater than the maximum offset across both of the slosh-disabled Monte Carlo analyses. The increase in docking offset (a function of attitude and position errors) can be attributed to the slosh disturbances and degradation in the RCS's precision when rejecting the disturbances. When the thrusters have a minimum on-time of 150 ms, 43% of the runs, at initial contact, failed to meet the IDSS IDD lateral RSS docking misalignment limits [ref. 2]. Therefore, the initial contact conditions resulting from the 150 ms on-times were not simulated with the docking model in Adams (see next section) since these cases are far outside of mechanism capability.

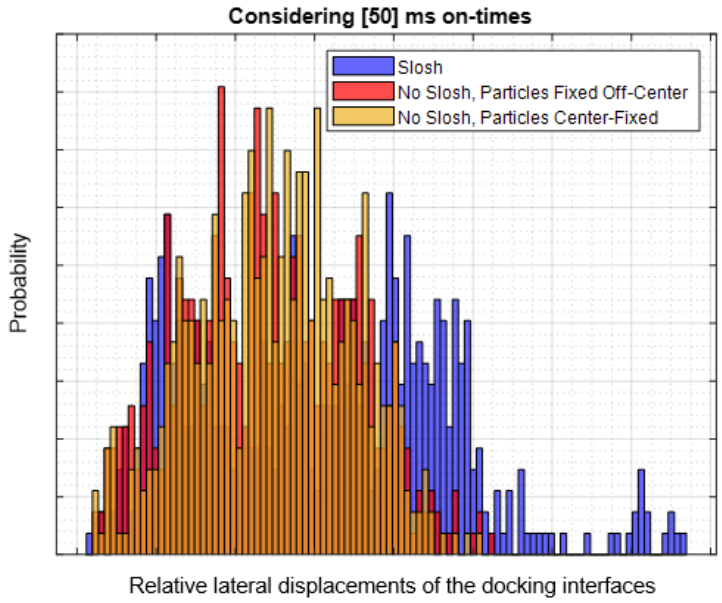

Figure 2.3-4. Relative Lateral RSS Misalignments of the Docking Interface with RCS Thruster Minimum On-Times of 50 ms

When IDSS limits are met and the chaser vehicle proceeds with docking, beginning of the capture sequence is critical for the docking mechanism because it transitions from an attenuation mode into a position control mode. To estimate the slosh forces in this duration, the maximum docking force on chaser vehicle was applied to the spacecraft. The distribution of forces sustained from the propellant sloshing through the entirety of this period is provided in Figure 2.3-5, which displays the number of simulations (y-axis) out of 2228 total runs in which the maximum combined (LOX and LCH_4) particle force met or exceeded the bin's force level (x-axis).

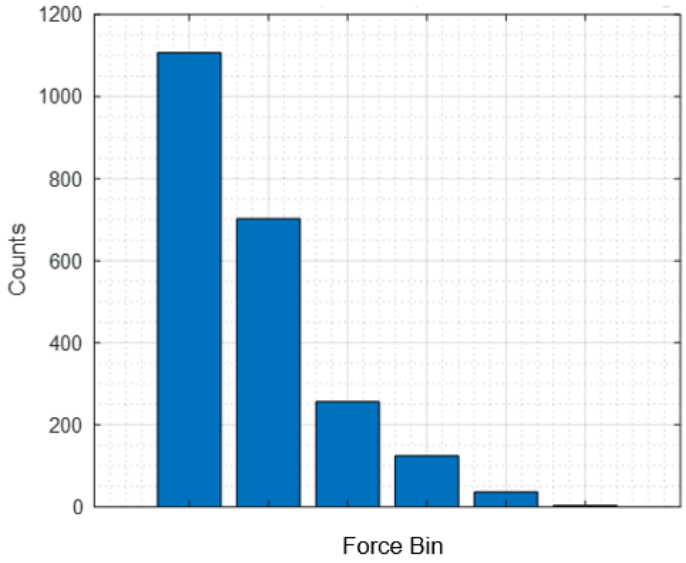

Figure 2.3-5. Distribution of the Combined Particle Slosh Force where the Force was Sustained During the Beginning of the Capture Sequence

The dynamic analysis of the chaser vehicle approach and docking was beneficial in identifying the sensitivity of the position/attitude accuracy at docking to the controller performance and RCS

thruster on-time. Figure 2.3-6 provides probability histograms outlining the relative lateral RSS docking misalignment values for each Monte Carlo simulation performed, for all thruster minimum on-times (50, 100, and 150 ms).

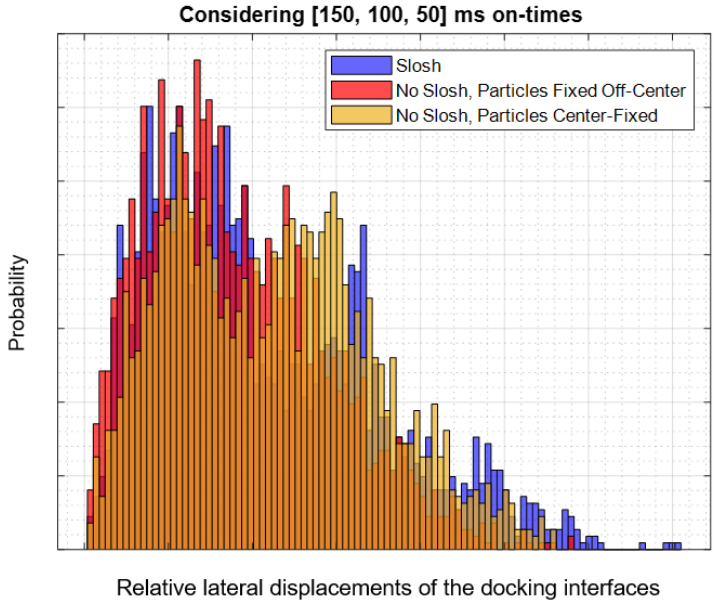

Figure 2.3-6. Relative Lateral RSS Misalignments of the Docking Interface Considering all Thruster Minimum On-times

Table 2.3-1 provides the relative change of the docking interface lateral offsets between the various Monte Carlo analyses. The offsets were the highest when slosh was enabled, with decreased instances for slosh disabled with propellant location bias, and further decreased instances were observed when slosh was disabled, and the masses assumed stationary along on the tank centerline. The maximum lateral velocities (not shown) are the highest when there is a constant propellant mass location bias (i.e., "slosh disabled with propellant offset" runs). Lateral velocities decreased comparatively when the slosh model was enabled and were even lower when the slosh was disabled (in the absence of a slosh mass location offset).

Table 2.3-1. Maximum Relative Changes of Docking Interface Lateral Offsets across all Scenarios and Monte Carlo Results

Thruster minimum on-time (ms)	**Lateral Offset Percent (%) Difference between Slosh Enabled and Slosh Disabled**	**Lateral Offset Percent (%) Difference between Slosh Enabled and Slosh Disabled with Propellant Offset**
150 ms	27.1%	23.2%
100 ms	40.4%	26.7%
50 ms	51.6%	48.1%

At docking, the force contribution from both the LCH_4 and the LOX particles generated a torque about the docking interface that was within the lowest NDSB2 soft capture load limit. These forces may also be sustained for tens of seconds.

The dynamic simulations discussed in this section provided preliminary information regarding the impact of propellant slosh on the chaser vehicle docking with the target vehicle. In addition, the

initial contact conditions from these simulations were used as an input for a higher fidelity docking mechanics simulation that is conducted using Adams.

2.4 Chaser/Target Vehicle Docking in Adams with the NDSB2

The final analysis performed was the simulation of the chaser/target vehicle docking in Adams with the test validated NDSB2 mechanism [ref. 1]. Figure 2.4-1 shows the active and passive components of the NDSB2 mechanism model.

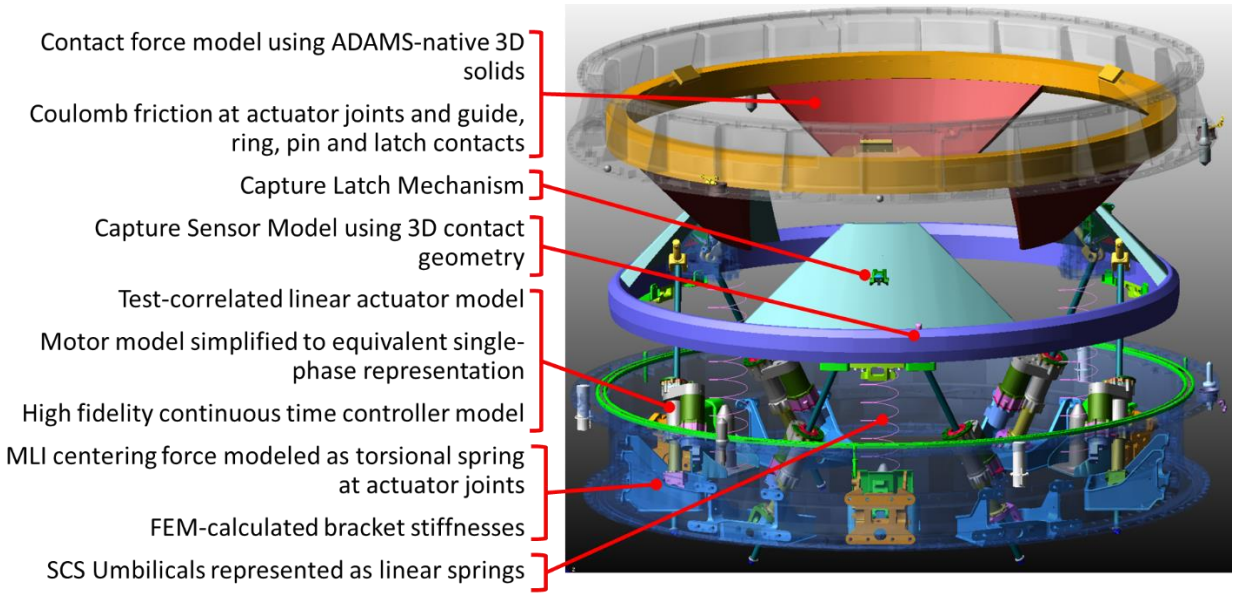

Figure 2.4-1. NDSB2 Dynamics Model

This is an automated system that allows an equipped chaser vehicle to dock with a target vehicle. The NDSB2 includes provisions for soft capture, structural attachment, power/data/fluid transfer, and undocking.

2.4.1 Docking Simulation Setup

In these simulations, the target vehicle was modeled as a rigid body. The simulated chaser vehicle also included the particle model used in the flight dynamics simulation to capture the effects of propellant slosh. Like the dynamics simulation, the docking simulation assumed each propellant has an equivalent mass fraction. The remaining inert mass of each propellant was assumed to be rigidly attached to the vehicle dry mass at the tank center. The forces on the chaser vehicle due to slosh were calculated using a Simulink sub-model and applied to the spacecraft at its dry CM. The Adams simulation, which includes the chaser vehicle and the target vehicle masses, a high-fidelity model of the NDSB2 mechanism, and the slosh particle model, integrates the equations of motion to determine the positions, orientations, rates, and accelerations of the chaser vehicle. Three run sets were performed, each limited to 100 cases due to computational complexity.

1. The *No Slosh* runs use the ICCs from the slosh-disabled dynamics simulation. All propellant mass was modeled as a point mass fixed at the tank geometric center, resulting in a pure rigid body representation of the chaser vehicle.

2. The *Slosh Enabled* runs use the ICCs and initial propellant states from the slosh-enabled dynamics simulation and have slosh particle models enabled after contact. The non-sloshing propellant was assumed to be fixed as a point mass at the tank center.
3. The *Slosh ICCs Only* runs use the ICCs from the slosh-enabled dynamics simulation, but slosh is disabled for the Adams simulation. At the beginning of the Adams NDSB2 docking simulation (i.e., at first contact), all propellant mass was modeled as a point mass that is fixed at the tank center.

2.4.2 Docking Simulation Results

The Adams simulation provided key information on the NDSB2 mechanism performance, namely: capture success, relative motions, and forces, torques, and moments on the mechanical system. There are limits for axial, lateral, angular velocities, and angular misalignments for the NDSB2 ICCs. As an example, Figure 2.4.2-1 shows the lateral and wobble misalignment ICCs with slosh enabled. *Wobble* refers to the angle between the chaser and target vehicle docking axes.

In this analysis, a docking was considered successful if all three capture sensors were persistently depressed (i.e., which indicates that the three soft capture latches have engaged successfully with the corresponding target vehicle passive features). The soft capture latch engagement and sensor confirmation must occur before the SCS linear actuators reach the end of their Lunge stroke as defined by a software limit. If the Lunge stroke limit is reached before the latches are engaged, then the NDSB2 firmware declares a missed capture, releases the soft capture latches, and signals the chaser vehicle to perform an automated retreat. Engagement of the soft capture latches triggers the start of attenuation, alignment, and retraction for hard capture operations. All the missed capture cases were from GNC simulations with a 100 ms minimum thruster on-time (recall the ICCs from the 150 ms on-times were simulated in Adams) with lateral misalignments outside of the ICC requirement.

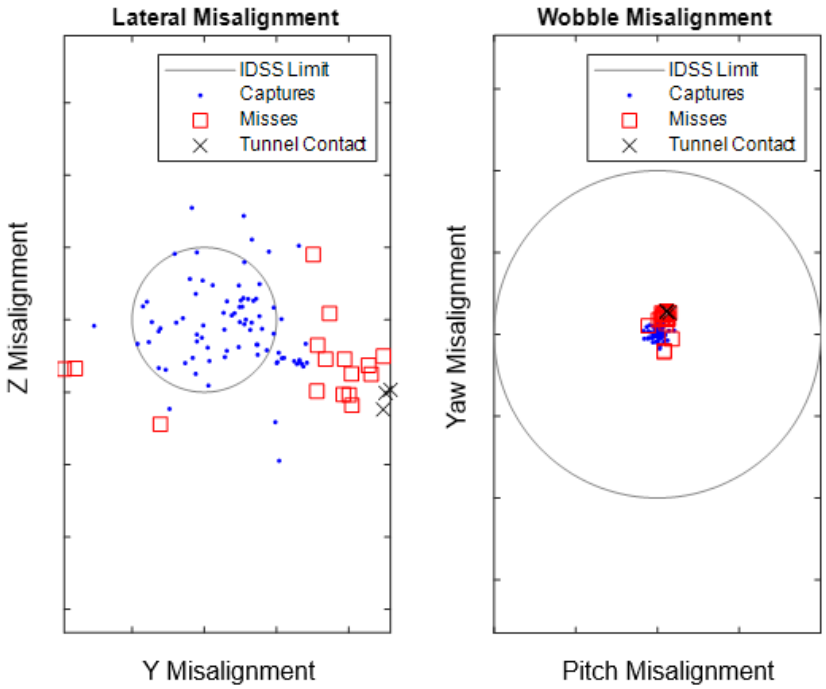

Figure 2.4.2-1. Lateral and Wobble Misalignment ICCs with Slosh Enabled

The soft capture interface loads during capture and attenuation, with and without slosh effects, are within NDSB2 docking mechanism design requirement limits [ref. 8] with margin. However, because un-modeled contact between the linear actuators and the hard capture tunnel would have occurred in some select *Slosh Enabled* cases, the additional loads may exceed interface load limits and result in damage to the SCS and support structures. The linear actuator joint angles are plotted against the vehicle relative dynamic motion (VRDM) and joint deadstick limits for the set of runs with slosh activated in Figure 2.4.2-2. On this plot, the black dots represent the actuator joint angles at one actuator at one time step in one of the docking simulations. Actuator motion was within acceptable limits for all cases in the *No Slosh* set. In the *Slosh Enabled* runs, three cases resulted in exceedance of the lower joint deadstick limits, indicating that the actuators would have contacted the surrounding structure (internal to the docking tunnel). These contacts were not modeled and are not included in the reported loads. Contact between an actuator and the surrounding structure can result in damage to the SCS and inability to re-attempt docking. All three cases that resulted in actuator-to-tunnel contact were among the 19 missed capture cases that were present in both the *Slosh Enabled* and *Slosh ICCs Only* sets. These results indicate that the actuator-to-tunnel contact was caused primarily by the extreme initial contact conditions rather than slosh forces after contact.

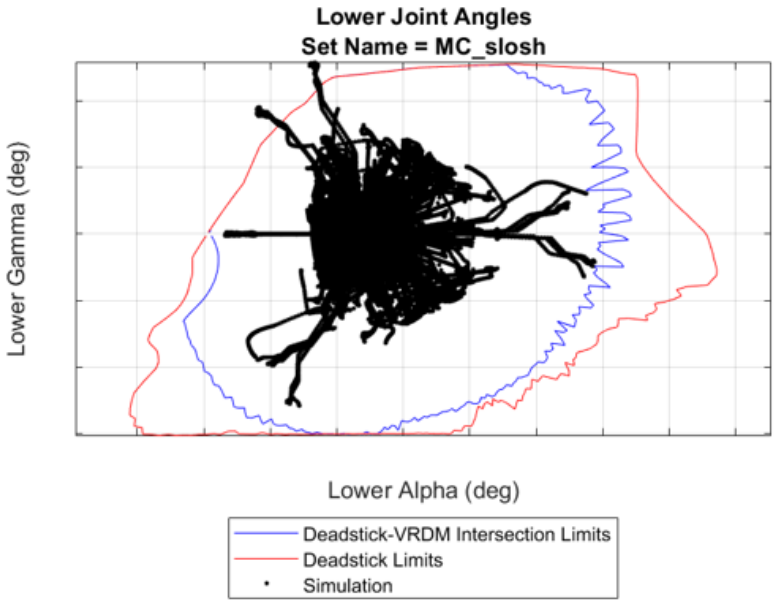

Figure 2.4.2-2. Linear Actuator Lower Joint Motion with Slosh Enabled

Figure 2.4.2-3 compares the maximum loads during soft capture as a percentage of limit load for all three run sets. These results show that the contribution of propellant slosh to overall capture and attenuation loads is small if tunnel contact loads are excluded. The maximum combined force magnitude from both the LCH_4 and LOX particles through all simulations was comparable to the forces observed from Dynamic Simulation analysis.

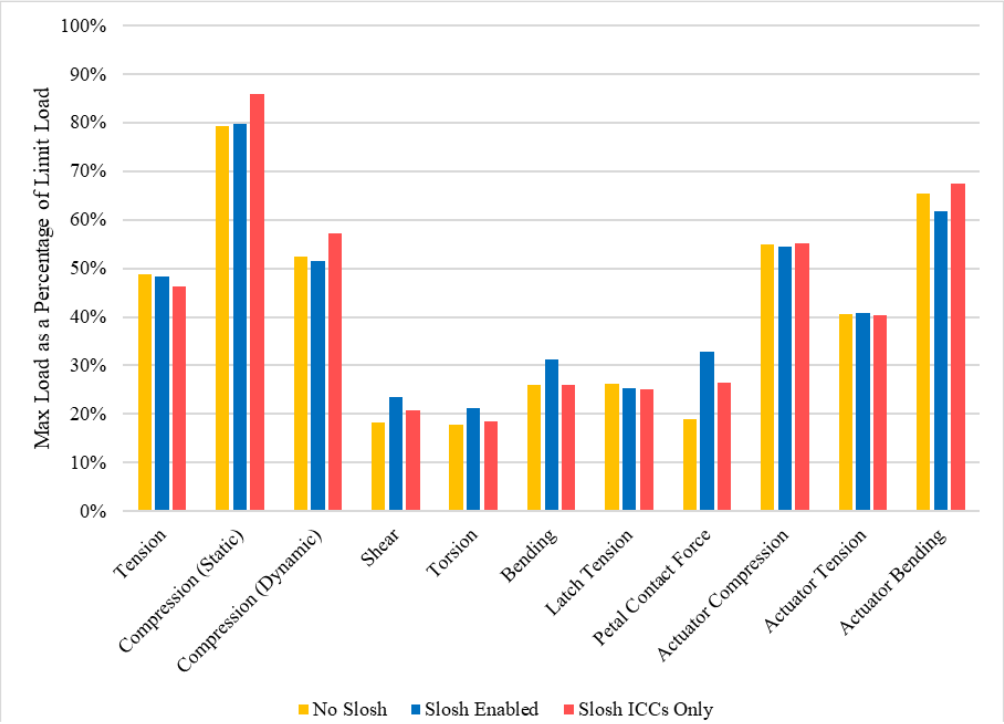

Figure 2.4.2-3. Soft Capture Loads as a Percentage of Limit Load

Figure 2.4.2-4 shows a comparison of the Hard Capture System (HCS) maximum engagement loads for all three run sets, including an assumed 1.25 uncertainty factor, as a percentage of the limit load. While the HCS load limits were not exceeded, it is noteworthy that slosh forces are present during hard capture, which is normally a quiescent period. This can be seen in Figure 2.4.2-5, which provides the axial forces from the LOX and LCH_4 particle slosh in the Slosh Enabled simulations. Table 2.4.2-1 summarizes the docking simulations results regarding docking success.

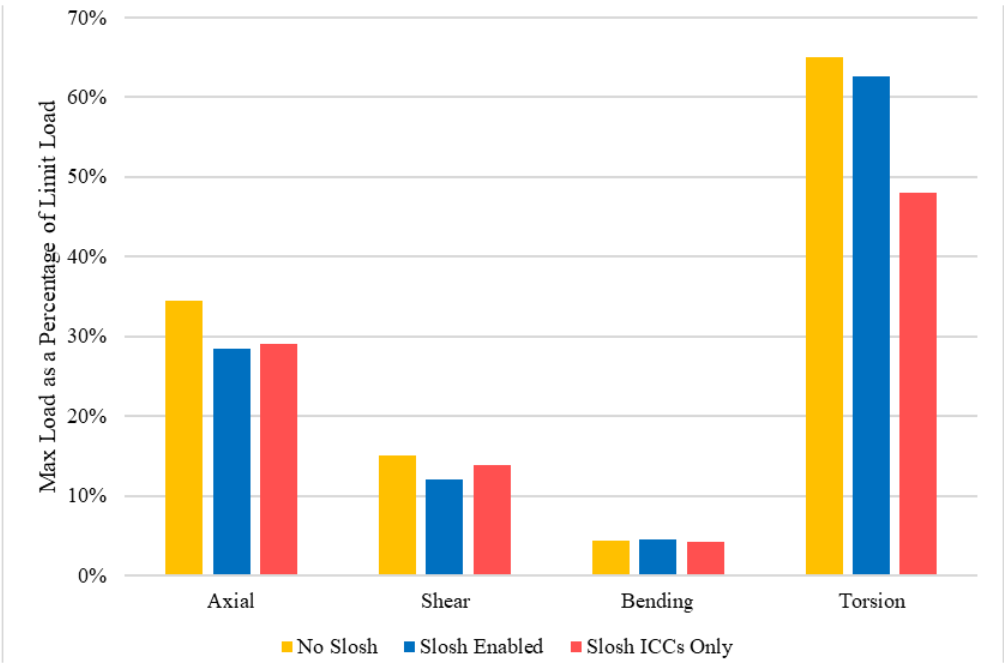

Figure 2.4.2-4. HCS Engagement Loads as a Percentage of Limit Load

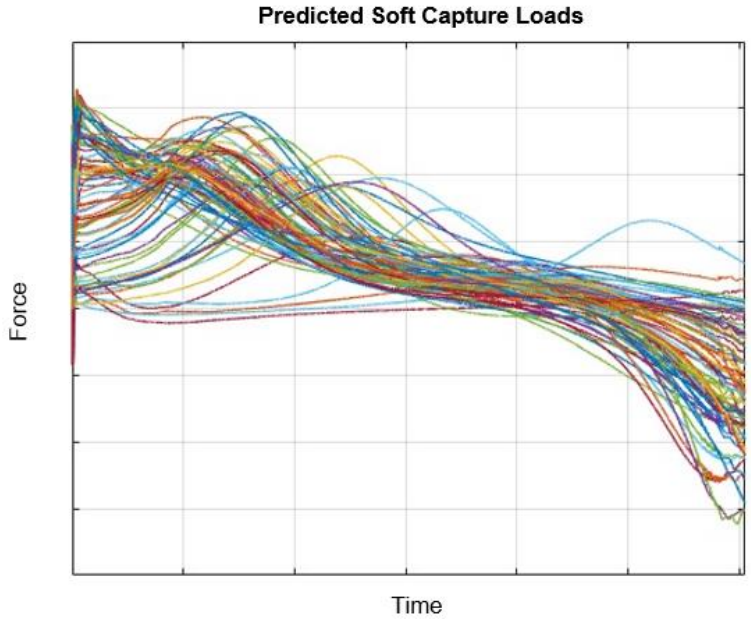

Figure 2.4.2-5. Predicted Soft Capture Loads

Table 2.4.2-1. Docking Success Summary

	No Slosh	**Slosh Enabled**	**Slosh ICCs Only**
Cases	100	100	100
Captures	83	81	81
Missed Captures	17	19	19
Improper Guide Meshing	0	4	4
Actuator to Tunnel Contact	0	3	3
Successful Completion of Docking (Hard Capture)	83	81	81

Figure 2.4.2-6 shows the ICC with the largest lateral misalignment of all the slosh-enabled cases. In this case, the SCS alignment guides are improperly meshed which precludes successful capture. This also introduces the risk of contact between an actuator and the surrounding structure that can damage the SCS and creates the inability to re-attempt docking.

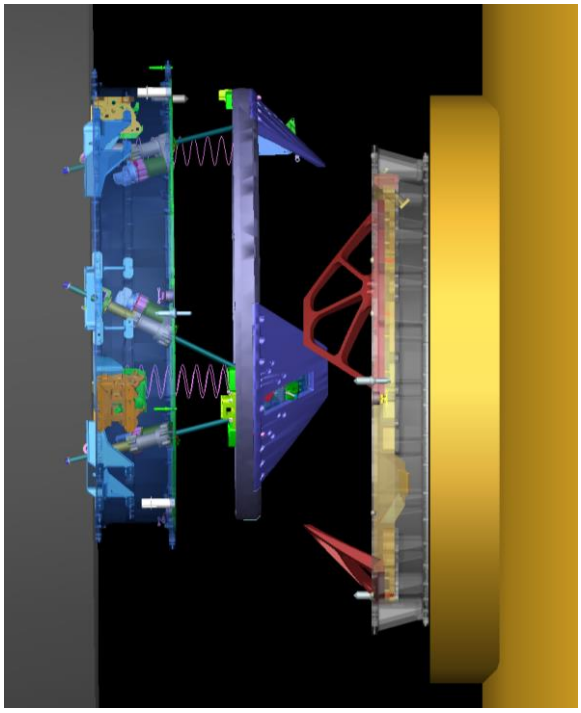

Figure 2.4.2-6. Severe Misalignment Case with Improper Guide Meshing

No docking failures were observed after successful capture in the Adams dynamic simulation of the chaser/target vehicle docking even with the presence of slosh forces. In the cases that capture was missed, it was a result of extreme relative lateral RSS misalignments of the docking interface (poor rigid body control performance) at first contact rather than post-contact slosh forces. The contribution of propellant slosh to overall capture and attenuation loads does not result in an exceedance of the NDSB2 SCS or HCS load limits, except for cases with actuator to tunnel contact loads.

2.5 Summary of Results

This section discusses the summary of results from (1) Fluid Mechanics, (2) Impulse/Momentum, (3) Dynamic Simulation with Slosh Particle Model, and (4) Docking Simulation with Slosh Particle Model. These four methods were implemented to directly assess the forces generated by the chaser vehicle LOX and LCH_4 low-g slosh and their relative magnitudes (see Figure 2.5-1). All the models made assumptions on the propellant slosh behavior which were not validated, as the fluid dynamic behavior in a low-g environment is an area of active research with limited data for model validation. The first method, the fluid mechanics approach, resulted in the lowest estimated forces. However, these forces can be sustained for a long duration (tens of minutes). The second method, the impulse/momentum approach, serves as an upper-bound on the predicted force over a short impact duration. The third methodology, the dynamic simulation with propellant slosh particle models, resulted in the second highest slosh force magnitudes during the approach. This analysis highlighted sensitivities to the RCS actuation capability and would be expected to vary with NRHO location in orbit, control design tuning, and approach profile variations. The fourth methodology, the docking simulation in Adams, represented the chaser vehicle and the target vehicle as rigid bodies and implemented the slosh particle model. This analysis verified the dynamic simulation results for slosh force magnitudes and was able to identify missed capture cases and scenarios that would be potentially damaging to the docking mechanism. This higher

fidelity model leveraged the same set of assumptions on the approach and vehicle dynamics (including the unvalidated slosh particle model), where the results may also vary depending on the docking hardware and subsequent parameter selection.

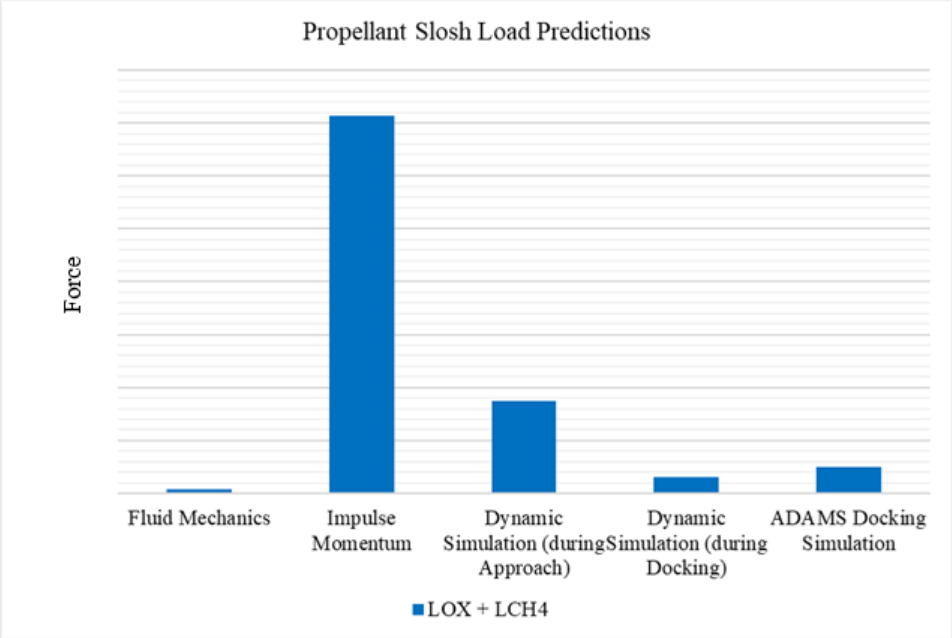

Figure 2.5-1. Propellant Slosh Load Predictions from Multiple Methods

3.0 Findings, Observations, and NESC Recommendations

3.1 Findings

F-1. The chaser vehicle propellant slosh forces were evaluated for multiple models/simulations:

a. The fluid mechanics approach using conservation of momentum resulted in the lower-bound slosh forces that can persist for tens of minutes.

b. The impulse/momentum approach from the combination of LOX and LCH_4 resulted in the upper-bound slosh force with an assumed short collision duration.

c. The dynamic simulation in Simulink with coupled fluid particle models in of LOX and LCH_4 estimated the second largest peak combined force during the chaser vehicle approach. Peak slosh forces during docking were sustained for tens of seconds.

d. The higher fidelity docking simulation in Adams exhibited slightly higher slosh force magnitudes compared to the dynamic simulation in Simulink, which was absent of a docking mechanism.

F-2. There was no observed correlation between the initial propellant location within the tank at the beginning of the docking approach and docking success.

F-3. The Adams simulation indicated that 19 (17) cases would fail to dock when propellant slosh was enabled (disabled) for the 100 hand-selected ICCs corresponding to RCS minimum on-times of 50 and 100 ms.

F-4. All the simulations where the chaser vehicle failed to dock to the target vehicle were due to the ICCs causing misalignments at time of docking rather than the post-contact, slosh-induced load.

F-5. The Adams docking simulations showed that there were no docking failures after soft capture latches engaged successfully, indicating that the mechanism can withstand post-capture slosh forces.

F-6. Extreme misalignments from the *Slosh Enabled* cases have improper guide meshing and linear actuator contact with the tunnel structure that may result in interface load limit exceedances, SCS damage, and the inability to reattempt docking.

F-7. The peak loads during soft capture did not exceed the NDSB2 load limits when actuator to tunnel contact loads were excluded and the contribution of post-contact propellant slosh to overall capture and attenuation loads is small.

F-8. The peak HCS engagement loads with an assumed 1.25 uncertainty factor are within the mated NDSB2 hard capture tunnel load capability.

F-9. Slosh disturbances persisted through ready-to-hook sensor activation and hard capture hook driving, which typically occur in a quiescent environment.

3.2 Observations

O-1. The original plan to evaluate propellant slosh forces alone during and just after docking would have been inadequate to evaluate capture success or the potential of incurring damage to the docking mechanism.

O-2. Propellant slosh degraded controller performance during the chaser vehicle approach simulations.

O-3. The particularly large moment arm between the chaser vehicle propellant tanks and the docking interface amplified the slosh force effects on misalignments and torques.

O-4. The dynamic simulation had cases where the propellant relative velocity due to the braking maneuver was sustained until docking.

O-5. The slosh modeling assumptions, notably the lumped mass and critically damped contact, were made to simulate the displacement of a cohesive slug of propellant and limited interactions with the tank wall. These assumptions break down when there are different fluid initial conditions, increased time horizons, and dynamic tank motions.

O-6. The propellant slosh particle model was tuned using CFD analysis but not validated using test data.

O-7. The Adams docking simulation excluded the dynamic simulation ICCs with 150 ms minimum thruster on-times since the lateral offset at time of docking exceeded the IDSS IDD limits for 43% of the cases ran when slosh was enabled.

O-8. The NDSB2 limits on VRDM were violated during the simulations performed with slosh enabled, indicating that there could be collisions external to the docking mechanism (i.e.,

appendages, solar arrays, or peripheral hardware near the docking mechanism) during soft capture. However, these limits are specific to NDSB2 and may be different if another docking mechanism is used on the chaser vehicle.

O-9. Aside from the IDSS interface load limits, the docking mechanism performance and limitations discussed in this report are specific to NDSB2 and may be different if another docking mechanism is used on the chaser vehicle.

3.3 NESC Recommendations

The following NESC recommendations are directed to anyone evaluating loads at docking for vehicles with a significant propellant mass fraction.

R-1. Account for the chaser vehicle propellant slosh in the GNC design and in determining the docking ICCs. ***(F-4, F-6, O-2)***

R-2. Include slosh effects in the verification of docking mechanism ready-to-hook sensor activation and hook closure. ***(F-9)***

R-3. Evaluate the sensitivity of docking success to the approach profile, and in particular the timing of the deceleration, to ensure propellant slosh is sufficiently attenuated prior to docking. ***(F-3, F-6, F-9, O-2, O-4, O-5)***

R-4. Validate propellant slosh model(s) for the chaser vehicle dynamic simulations with test data. ***(O-5, O-6)***

R-5. Advance slosh models to expand the range of conditions under which it can accurately model propellant loads. ***(O-5, O-6)***

4.0 Alternate Technical Opinion(s)

No alternate technical opinions were identified during this assessment by the NESC assessment team or the NESC Review Board (NRB).

5.0 Other Deliverables

No unique hardware, software, or data packages, other than those contained in this report, were disseminated to other parties outside this assessment.

6.0 Recommendations for the NASA Lessons Learned Database

No recommendations for NASA lessons learned were identified as a result of this assessment.

7.0 Recommendations for NASA Standards, Specifications, Handbooks, and Procedures

No recommendations for NASA standards, specifications, or procedures were identified as a result of this assessment.

8.0 Definition of Terms

Finding	A relevant factual conclusion and/or issue that is within the assessment scope and that the team has rigorously based on data from their independent analyses, tests, inspections, and/or reviews of technical documentation.
Lesson Learned	Knowledge, understanding, or conclusive insight gained by experience that may benefit other current or future NASA programs and projects. The experience may be positive, such as a successful test or mission, or negative, as in a mishap or failure.
Observation	A noteworthy fact, issue, and/or risk, which is not directly within the assessment scope, but could generate a separate issue or concern if not addressed. Alternatively, an observation can be a positive acknowledgement of a Center/Program/Project/Organization's operational structure, tools, and/or support.
Recommendation	A proposed measurable stakeholder action directly supported by specific Finding(s) and/or Observation(s) that will correct or mitigate an identified issue or risk.

9.0 References

1. EID684-17555 NDSB2 Dynamics Model Correlation Report, 2021.
2. International Docking System Standard (IDSS) Interface Definitions Document (IDD), Revision F, 2022.
3. Kane, T. R., and Levinson, D. A., *Dynamics: Theory and Applications*, McGraw-Hill, New York, 1985.
4. NESC Assessment TI-12-00766, Exploration Systems Independent Modeling and Simulation, "Multi-Purpose Crew Vehicle/Interim Cryogenic Propulsion Stage Separation Analysis Artemis 2 MAC-2 Update," Stakeholder Briefing, 12 January 2023.
5. 683-104065, NDSB2 Linear Actuator System Envelope Drawing.
6. Storey, J., Kirk, D., Marsell, B., and Schallhorn, P., "Progress Towards a Microgravity CFD Validation Study Using the ISS SPHERES-Slosh Experiment," AIAA Propulsion and Energy 2020 Forum, *In-Space Liquid Propulsion System Development*, August 24-28, 2020, Virtual Event.
7. SSP-51075 Rev. D, NASA Docking System Block 2 Interface Definitions Document.
8. Starr, Brett, VanZwieten Cook, Tannen, Benson, William, Pei, Jing, Storey, Jedediah, Marsell, Brandon, Lee, Esther, and Elke, William, "Evaluation of Low Gravity Propellant Motion Experiments for Validation of Spacecraft Slosh Models," AAS-25-174, *AAS Guidance, Navigation and Control Conference*, Breckenridge, CO, January 31 – February 5, 2025.
9. Elke, William, Bell, John, McFatter, Justin, and Pei, Jing, "Implementation of a Slosh Mechanical Model during Spacecraft Approach and Docking," AAS-25-173, *AAS GN&C Conference*, Breckenridge, CO, January 31 – February 5, 2025.